separations

Review

Advances in Cork Use in Adsorption Applications: An Overview of the Last Decade of Research

João Jesus [1], Raquel Nunes da Silva [1] and Ariana Pintor [2,3,*]

[1] CTCOR-Cork Technological Centre, Rua Amélia Camossa, 4536-904 Santa Maria de Lamas, Portugal; jjesus@ctcor.com (J.J.); rsilva@ctcor.com (R.N.d.S.)
[2] Laboratory of Separation and Reaction Engineering-Laboratory of Catalysis and Materials (LSRE-LCM), Department of Chemical Engineering, Faculty of Engineering, University of Porto, Rua Dr. Roberto Frias, 4200-465 Porto, Portugal
[3] ALiCE-Associate Laboratory in Chemical Engineering, Faculty of Engineering, University of Porto, Rua Dr. Roberto Frias, 4200-465 Porto, Portugal
* Correspondence: ampintor@fe.up.pt

Abstract: Cork-based adsorbents have been gathering interest from the research community since the 1990s. A first review was published on this topic in 2012. Still, in the last decade, novel activated carbons and biochars, in multiple applications, have been produced using cork as a raw material. This review presents these novel insights into the properties of cork, in its various forms, and how they relate to adsorption capacity. Details on new preparation methodologies and respective characteristics of cork-based activated carbons and biochars are thoroughly compared, and patterns are identified. Finally, the adsorption capacity of these materials in experimental conditions is reviewed for different compounds: heavy metals, organics, and gaseous pollutants. This review provides a complete picture of the kind and quality of different cork forms, their relative economic value, and how their conversion into activated carbons and biochars can contribute to a more circular economy by producing adsorbents that aid in the reduction of multiple pollution types.

Keywords: cork; biochar; activated carbons; adsorption

Citation: Jesus, J.; Nunes da Silva, R.; Pintor, A. Advances in Cork Use in Adsorption Applications: An Overview of the Last Decade of Research. *Separations* **2023**, *10*, 390. https://doi.org/10.3390/separations10070390

Academic Editor: Dimosthenis Giokas

Received: 31 May 2023
Revised: 23 June 2023
Accepted: 26 June 2023
Published: 3 July 2023

1. Introduction

Cork, the bark of the cork oak (*Quercus suber* L.), is one of nature's most unique and interesting materials. Its most common use is to produce cork wine stoppers, but during this process, about 80% of the raw material is rejected as a byproduct [1], thereby calling for a valorization by incorporation in added-value products. The most common of those are expanded corkboard, agglomerates, and composites, typically used for boards and insulation for floors and walls. However, new cork-based materials are being developed by the day, including novel composites and innovative applications in product design [2].

A matter of particular interest is the application of cork byproducts in environmental technology, namely the valorization of its less valuable waste, cork powder, which corresponds to 25% in weight of the original cork material extracted from the tree. A decade ago, Pintor et al. [3] published the first publication with an overview of the applications of cork powder and granulates in adsorption processes for the decontamination of water and air, including its transformation to cork-based activated carbons. In the first decade of the 2000s, research on cork products increased almost linearly year to year, and investment in cork R&D increased substantially.

The 2010s have shown that the number of research results cannot continue to grow indefinitely if sound quality is to be maintained: although the trend in publications with the "cork" keyword is still increasing, the rate of increase has slowed down considerably (Figure 1). A peak in Scopus-indexed publications was registered in 2019, but the number of publications reported so far in 2022 represents only a 15% increase from 2011.

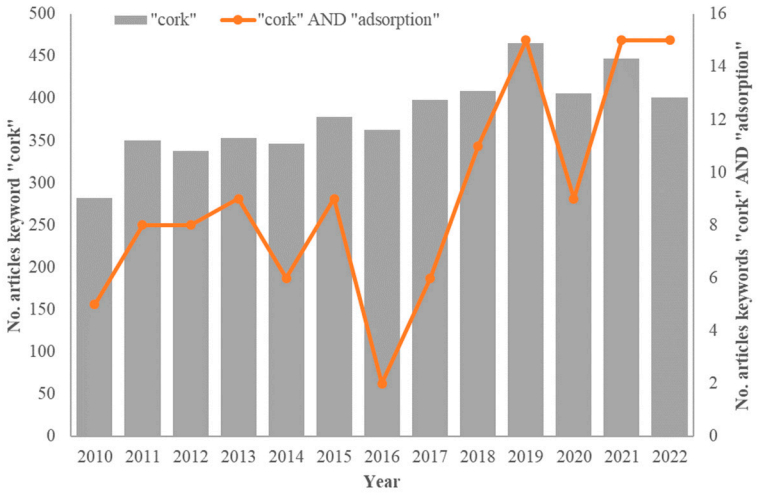

Figure 1. Evolution of the number of publications on Scopus-indexed journals containing the keywords "cork" or both "cork" and "adsorption" between 2010 and 2022.

On the other hand, more publications can be found on the topic of adsorption using cork-based materials (represented in Figure 1 by Scopus-indexed publications with the keywords "cork" AND "adsorption"), especially in the last five years. New trends have emerged in the production of biochar and activated carbons from cork, and innovative applications for these materials have been initiated. The environment is more and more a "hot topic", with many avenues in research to be pursued, and cork is a material of choice in this regard, given the often-claimed carbon-negative status of the products of its industry.

This work aims to update the state-of-the-art on cork and cork-derived materials in adsorption applications in the last decade. The new trends will be critically overviewed and analyzed, considering future avenues of work.

2. Brief Description of Cork Industrial Processes and Implications on Material Quality

Cork is extracted from the trunk and main branches of the *Quercus suber* L. tree in semi-tubular shapes, usually in the end of Spring and beginning of Summer, with proper care to not harm the tree, which is intended to recover and regrow cork [4].

The first cork extraction from each tree—roughly 25 years after plantation—is designated as 'virgin', which is deemed too irregular for cork stopper production. After 9 years of cork regrowth, the first reproduction cork is obtained, which is named 'secundeira' and is still too irregular. Only after at least 9 more years is obtained a higher quality reproduction cork, called "amadia". The cycle is repeated every 9 years up to 200 years per tree, depending on its lifespan [4]. Furthermore, from the pruning of smaller tree branches, 'falca' is extracted—a mixture of cork, inner bark, and wood [5].

Several waste materials resulting either from the extraction process in the 'montado' (the cork oak forest) itself—cork of low quality due to its low thickness or due to having been attacked by fungi or insects—or from the processing operations—faulty cork stoppers, remains of the punching process, and others—are used to produce granulates of varying densities and qualities.

In summation, "amadia" cork is used for natural cork stopper production. Virgin cork and the different types of waste mentioned above are granulated into millimeter-sized particles and can be upcycled into other cork-derived products. The most common application is to produce composite agglomerates (also known as white agglomerates) bound together by a synthetic bonding agent (polyurethane), which can also be mixed with materials such as rubber, cement, and others. These agglomerates provide several commercial products, such as floorings or agglomerated cork stoppers [6].

On the other hand, 'falca' and even burned cork are used directly without boiling to produce expanded agglomerate, also known as black agglomerate, as 'falca', when

compared to other cork types, has a higher concentration of extractives which act as a natural adhesive. These materials can be expanded by being placed in autoclaves at 300–370 °C with no additives. This black agglomerate is more often used to produce thermal and acoustic insulation [7].

All these processing steps and production lines often produce cork powder, which can be used as a raw material in cork agglomerates production, but most of it is used in energy recovery processes for heating [5]. As they are the result of varying qualities of cork, different types of powder are likely to have different characteristics, although how this can affect its use as a biosorbent is currently, to the best of the authors' knowledge, unclear. More studies should be conducted to clarify if mixing powder from different sources is ultimately detrimental to its quality as a sorbent.

Another waste from the cork industry relates to the end-of-life of its products, i.e., used cork stoppers and used construction materials. These materials can potentially have more applications in biosorbent development when compared to powder, as they can be milled to the desired granulometry. However, they are likely to consist of a mixture of natural cork composites and stoppers with cork composites with other materials, such as rubber or agglomerated cork stoppers, with adhesives that might negatively impact the potential use as a sorbent.

Therefore, cork powder, preferably without adhesives, is the most likely candidate as a raw material for novel applications, due to its low cost and high-volume production within the industry, with little to no competing use. 'Falca', however, also has unique characteristics of a higher concentration of extractives, self-adhesive properties, and a lower price than almost any other raw material from the 'montado'. Therefore, it should also be considered for further research, as there might exist a possibility of economic feasibility and incentive if the prepared biosorbent is of sufficient quality and market price.

3. Novel Insights into the Properties of Cork and Cork Powder

A detailed review of cork and cork powder characteristics can be found in prior publications such as [3] and elsewhere [8]. Therefore, this section aims to provide a short summary along with an exploration of novel research that may provide new insights into the potential of this material.

H. Pereira in 2013 [9] determined the chemical composition of cork based on extensive sampling efforts of 29 provenances from six different production regions in Portugal, taken at cork stripping (Table 1).

Table 1. Mean, standard deviation and coefficient of variation (%CV) of chemical composition data for all cork samples [9].

	Parameter (% Oven-Dry Cork)	Mean ± Stdev	%CV
Extractives	Dichloromethane	5.8 ± 0.8	13.8
	Ethanol	5.9 ± 3.0	50.8
	Water	4.5 ± 1.6	35.6
	Total	16.2 ± 3.9	24.1
Suberin	Long chain lipids (LCL)	41.0 ± 5.2	12.7
	Glycerol (Gly)	3.8 ± 0.6	15.8
	Ratio LCL: Gly	11.3 ± 1.6	14.2
	Total	42.8 ± 6.2	14.5
Lignin	Klason lignin	21.1 ± 3.3	15.6
	Acid soluble lignin	0.9 ± 0.2	22.2
	Total	22.0 ± 3.3	15

H. Pereira concluded that there is a high variation between different trees. However, a more intense comparison between two particular regions did not find significant differences

between regions, with the exception of small magnitude differences in ethanol and water extractives and suberin content.

In that study, a ratio of suberin to lignin content was estimated at a mean value of 2.0 ± 0.4, an important ratio as each of these polymers provides different mechanical and physical behaviors in cells, translating to different compression resistance as well as recovery after stress. The polymers are also likely to have different impacts on the permeation and diffusion of liquids and gases through cork [9].

For further characterization and visualization of cork and cork powder, particularly their physical characteristics, scanning electron imaging (SEM) has been extensively used in the past. However, more recently, Lagorce-Tachon et al. [10] developed and automated an image processing analysis, thereby providing statistical distributions of useful structural properties such as cell size and wall thickness. This method can provide the geometrical characteristics of each cell and its walls (Figure 2) and has the potential to be used to study, in more detail, the mass transfer of gases such as oxygen through cork structure, which is relevant to cork stopper industry but also to newer applications such as pollutant gas adsorption.

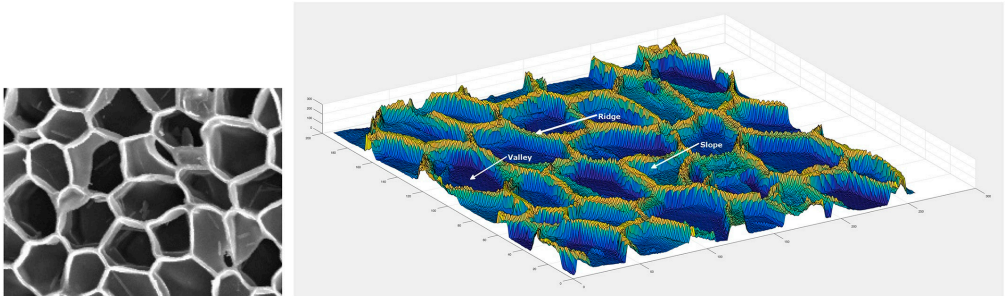

Figure 2. SEM image of a cross-section of cork cells (**left**) and corresponding 3D colored surface after analysis (**right**). Reprinted with permission from Lagorce-Tachon et al. [10]. Copyright © John Wiley and Sons, 2017.

Transmission electron microscopy (TEM) has also been recently applied to cork [11] as it can detect cell structures at a nanoscale, more specifically, in the case of cork, plasmodesmata (Figure 3)—thin channels with a diameter of ∼50 nm which cross cell walls, an important structure to understand the mechanisms of gas diffusion across cork cells.

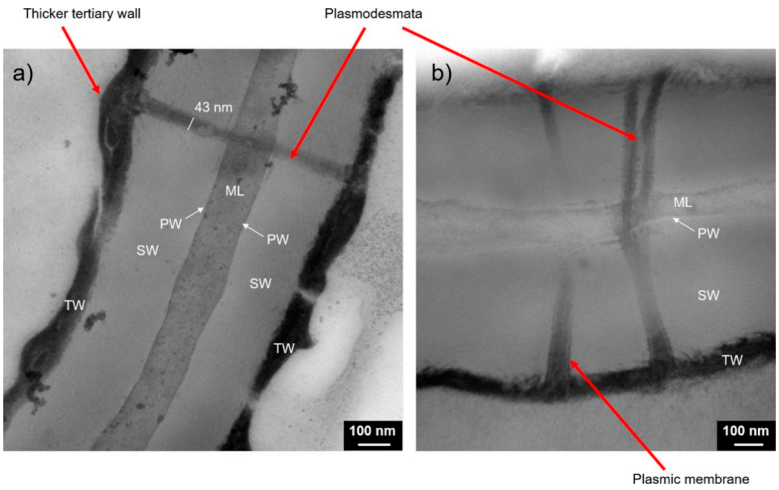

Figure 3. TEM images with detailed nanostructures such as plasmodesmata [11].

More advanced techniques have also been applied, such as neutron radiography and tomography [12] and X-ray tomography [11].

Although both these studies focused on cork stopper characterization and use in quality control, its application in cork powder characterization is yet unknown to the best of the authors' knowledge. With other materials, X-Ray tomography has been used to study the behavior of adsorption filters [13], while neutron imaging can be used to quantify the diffusion of ions inside porous materials [14].

Furthermore, although there are several studies detailing cork characteristics and quality in its natural state, very few studies focus on the physical characteristics of this material after reduction in size due to industrial processing, namely down to cork granulates and cork powder. Motte et al. in 2017 [15] studied the impact of milling on cork characteristics and found that between 200 and 350 µm, 80% of loaded density and elastic recovery is maintained compared to coarser cork particles. However, for cork powder (in this case defined as below 200 µm), there is an increase of packing density up to 30% and a reduction of elastic recovery between 35–40%. It was also found that the chosen milling technology significantly impacts the produced granule or powder. The same can apply to cork characteristics relevant to pollutant adsorption and should be investigated further. Although a significant portion of cork powder is a byproduct, cork granulates are produced by milling lower-quality cork or recycled materials.

Finally, it is important to note that cork exhibits high variability related to its origin and growing conditions. Cork powder, as a waste material, can present even higher variability as it can originate from a variety of production facilities and processes (cork stoppers, insulation, and other cork products with other chemicals mixed in) and from recycled materials.

4. Production of Activated Carbons and Biochars

The production of cork-based activated carbons had already been verified in the first decade of this century through the application of standard physical and chemical activation processes [3]. The most recent research, especially in the last four years, has focused on three main goals:

- Attempting the valorization of cork biomass from different origins (particularly cork powder);
- Reducing production costs for the valorization of waste biomass—mainly through the generation of biochars, skipping the activation step;
- Producing activated carbons with larger surface area and pore volume, honing their characteristics for their application.

4.1. Valorization of Different Types of Cork Biomass

Regarding the first point, researchers have produced both activated carbons and biochars using new biomass streams beyond cork powder and granulates. It is essential to experimentally verify the applicability of thermal treatment and activation procedures in different types of raw biomass since they may result in carbon products with varying textural and surface characteristics, even when their biological source is the same. In particular, Bhatia et al. [16] and Xu et al. [17] have used ground cork directly obtained from wine stoppers. The testing of these products is vital for their valorization after use because they may introduce some impurities in the precursor material. Atanes et al. in 2012 [18] highlight that waste cork powder may contain substances such as sulphamic acid, hydrogen peroxide, sodium hydroxide and polyurethane glue that are also used in manufacturing.

In 2014, Mestre et al. [19] used regranulated cork (produced industrially by hydrothermal treatment at around 350 °C for 20 min) as a precursor for activated carbon production. They determined that this raw material needed higher activation temperatures to achieve similar characteristics as the direct activation of conventional 'raw cork'. Some researchers have also studied the thermal transformation of cork products from *Quercus cerris* [20,21] and *Quercus variabilis* [22], which are slightly different from the traditional *Quercus suber*.

4.2. Production of Cork Biochars

The study of the thermal degradation of cork products and the search for low-cost methodologies for managing and valorizing waste have led to the rise in studies of cork biochar production. Cork has advantages as a raw material for biochar production due to its unique cellular structure [23] and the fact that it yields liquid pyrolysis products that can be recovered with added value [24]. Table 2 summarizes the methodologies reported in the literature for producing cork biochars when evaluated for their surface area and pore volume.

Table 2. Specific surface area and pore volume of cork biochars reported in the literature, along with the methodology details for their production by pyrolysis.

Source	Raw Material	Gas Flow	Heating Rate	Temperature Level	S_{BET} (m^2/g)	V_p (cm^3/g)
[18]	Cork powder (<0.17 mm)	N_2, 100 mL·min^{-1}	5 °C·min^{-1}	750 °C, no hold	7	0.01
[23]	Cork granulates (0.25–0.45 mm)	N_2, 300 mL·min^{-1}	10 °C·min^{-1}	450 °C, hold 30 min	32	0.04
				550 °C, hold 30 min	220	0.23
				650 °C, hold 30 min	322	0.24
				750 °C, hold 30 min	393	0.24
				550 °C, hold 1 h	245	0.24
				550 °C, hold 1.5 h	266	0.24
				550 °C, hold 2 h	275	0.24
[16]	Waste cork stoppers	N_2	10 °C·min^{-1}	600 °C, 2 h	448	0.04
[17]	Cork stoppers pulverized to <900 µm	N_2, 100 mL·min^{-1}	5 °C·min^{-1}	800 °C, 1 h	369	0.23
[25]	Cork granulates (0.25–0.45 mm)	N_2		550 °C, 1 h	379	0.17
[26]	Cork granulates (0.25–0.45 mm)	N_2, 100 mL·min^{-1}	10 °C·min^{-1}	150 °C, hold 90 min	2	0.01
				200 °C, hold 90 min	2	0.01
				250 °C, hold 90 min	3	0.01
				300 °C, hold 90 min	3	0.01
				350 °C, hold 90 min	4	0.01
				400 °C, hold 90 min	5	0.01
				450 °C, hold 90 min	31	0.03
				500 °C, hold 90 min	210	0.12
				550 °C, hold 90 min	489	0.27

The transformation process of cork biomass has been studied through thermogravimetric analysis [18] and the production of biochars at different temperature levels with an examination of gaseous and solid products [26]. Three stages were identified during temperature increase in cork pyrolysis:

- a first stage up to 200 °C, in which no chemical reactions were apparent and only moisture loss was observed;
- a second stage from 200 to 430 °C, which corresponded to the degradation of the main chemical components and the largest mass loss;
- a later phase between 430 and 550 °C, identified as volatilization of residual lignin and unstable carbon.

Over 550 °C, the degradation of cork's components is complete, and only the aromatic carbon structure remains, forming an amorphous char [23,26].

The main polysaccharides, hemicellulose, and cellulose are lost at the lower temperature range in the second stage [16,26]. The mass loss at this stage occurs mainly between 300–400 °C, the range of temperature at which the degradation of suberin, cork's main component, occurs [26]. Şen et al. and Nobre et al. [20,21], in their study on *Quercus cerris* biomass, have detected an increase in the thermal stability of biomass, reflected in the solid

char yield, with the increased suberin content in cork-rich biomass, when compared to phloem-rich biomass, whose main components are lignin and polysaccharides. However, other authors argue that the carbonization of cork at temperatures around 350 °C causes the evaporation and leaching of suberin, decreasing the thickness of the cork cell layer [24]. Although lignin degradation starts at lower temperatures, it is only fully degraded at a higher level, and therefore it may have a higher biochar formation ability than suberin, even though it is less thermally stable [26].

There are three types of pyrolysis for biomass valorization: torrefaction, which is carried out at low temperatures and short residence times; carbonization, which is performed at higher temperatures than torrefaction and long residence times; and fast pyrolysis, which runs at high temperatures and short residence times [21]. In the case of cork, it is clear that carbonization yields the best results in terms of the characteristics of the solid product since porosity is only developed over 450 °C, with pyrolysis times over 30 min [26].

These results are in line with other biochars produced from lignocellulosic biomass, which is the natural carbonaceous material of choice if the aim is to achieve high BET surface area and pore volume [27,28]. Biochar from lignocellulosic feedstock can achieve BET surface areas over 500–600 $m^2 \cdot g^{-1}$ at high enough temperatures (800–900 °C) [27,29]. More intermediate pyrolysis temperatures often yield BET surface areas in the range of 300–500 $m^2 \cdot g^{-1}$ [27,29,30], as reported for cork (Table 2). Cork is unique from other lignocellulosic materials due to its suberin content, which is not only interesting to recover as a liquid byproduct of carbonization [24] but also influences the thermochemical decomposition profile, which is governed by cellulose and lignin in the other materials of this category [29].

Recently, some other studies have used animal manure and algae as feedstocks for biochar production, but they yield carbons with much lower surface area, often below 100 $m^2 \cdot g^{-1}$, even at high temperatures [27,29].

Biochars from cork produced at lower temperatures have been deemed similar to lignite or coal and can be used as fuels with enhanced performance [20]. Another possible application of cork biochars is as soil amendments, although in this case, the increase in temperature may be beneficial since it increases the nutrient content and decreases the leaching of phenolic compounds to water, which may be toxic to plants [20,21].

4.3. Activation and Functionalization

Even though the properties of biochars are attractive for a variety of applications, they are less satisfactory for more specialized uses, such as the fabrication of activated carbon electrodes [31,32] and the adsorption of specific compounds for which the textural characteristics are determining, such as the narrow microporosity in the uptake of CO_2 [20]. High surface areas and pore volumes can only be achieved through more complex activation procedures, which can be either physical or chemical [18,32].

Recent advances in the production of activated carbons from lignocellulosic biomass propose a two-step process: the first pyrolysis is carried out at low temperature to produce biochar, and the second step is the activation of this biochar using physical or chemical processes [27]. In the case of cork, two-step processes have been reported in which the pretreatment consists of hydrothermal treatment [22,32] or slow pyrolysis [17,24,33,34]. Such a pretreatment enables the achievement of much larger surface areas and pore volumes after the activation step [17,24,25,34] and allows for the use of more environmentally friendly methodologies that minimize reactant consumption and energy expenditure [22]. Other innovative approaches include substituting aggressive basic agents like NaOH and KOH with lower impact reactants with similar effects, like $KHCO_3$ [32] or alternative alkalinity sources such as paper and pulp wastewater [35].

Table 3 shows the latest two-step activation processes described in the available literature and their results regarding the textural properties of the cork-based activated carbons or carbon nanoflakes.

Table 3. Specific surface area and pore volume of cork-based porous carbon materials reported in the literature, along with the methodology details for their production.

Source	Raw Material	Pretreatment	Activation Agent	Pyrolysis Conditions	S_{BET} (m^2/g)	V_p (cm^3/g)
[33]	Cork granules	Carbonization under N_2, 400 °C, 1 h	CO_2	10 °C·min^{-1} to 800 °C, hold until burn-off 26%	581	0.38
				10 °C·min^{-1} to 800 °C, hold until burn-off 49%	839	0.63
[18]	Cork powder (<0.17 mm)		CO_2	N_2, 100 mL·min^{-1}, 5 °C·min^{-1} to 750 °C, switch to CO_2, hold 2 h	76	0.06
			KOH 1:1 w/w, impregnation	N_2, 100 mL·min^{-1}, 5 °C·min^{-1} to 750 °C, no hold	584	0.33
[19]	Regranulated cork (2.0–2.8 mm)	Hydrothermal carbonization, ~350 °C, 20 min (before study)	Steam	N_2, 480 mL·min^{-1}, 10 °C·min^{-1} to 800 °C, hold 1 h	750	0.50
	Regranulated cork (0.5–1.0 mm)		KOH 1:1 w/w, impregnation	N_2, 300 mL·min^{-1}, 10 °C·min^{-1} to 700 °C, hold 1 h	729	0.35
				N_2, 300 mL·min^{-1}, 10 °C·min^{-1} to 800 °C, hold 1 h	948	0.47
			KOH 2:1 w/w, impregnation	N_2, 300 mL·min^{-1}, 10 °C·min^{-1} to 700 °C, hold 1 h	874	0.41
			K_2CO_3 1:1 w/w, impregnation	N_2, 300 mL·min^{-1}, 10 °C·min^{-1} to 700 °C, hold 1 h	617	0.29
				N_2, 300 mL·min^{-1}, 10 °C·min^{-1} to 800 °C, hold 1 h	907	0.42
			K_2CO_3 2:1 w/w, impregnation	N_2, 300 mL·min^{-1}, 10 °C·min^{-1} to 700 °C, hold 1 h	604	0.30
[31]	Cork granules		KOH 1:1 w/w, impregnation	Ar, 300 mL·min^{-1}, 800 °C, 2 h	881	0.52
			KOH 2:1 w/w, impregnation		1082	0.66
			KOH 3:1 w/w, impregnation		916	0.54
[35]	Cork granulates (0.5–1.0 mm)		10 M NaOH and alkaline wastewater, 50:50 v/v, impregnation 0.8 g/50 mL	N_2, 5 °C·min^{-1} to 150 °C, 10 °C·min^{-1} to 900 °C, hold 30 min	1670	1.14
[32]	Cork granules	0·5 M H_2SO_4 + distilled water, hydrothermal carbonization at 160 °C for 2 h	$KHCO_3$ 1:1	Ar, 850 °C, 2 h	1057	0.64
[22]	Cork granules from *Quercus variabilis*	Hydrothermal treatment at 180 °C, 5 h		N_2, 100 mL·min^{-1}, 800 °C, 1 h	376	0.20
		Hydrothermal treatment at 180 °C, 5 h; carbonization under N_2, 100 mL·min^{-1} 800 °C, 1 h	Air	350 °C, 1 h	404	0.23
				400 °C, 1 h	540	0.33
				450 °C, 1 h	580	0.38

Table 3. *Cont.*

Source	Raw Material	Pretreatment	Activation Agent	Pyrolysis Conditions	S_{BET} (m^2/g)	V_p (cm^3/g)
[24]	Cork powder (< 0.18 mm)	Carbonization under N_2, 10 °C·min^{-1} to 350 °C, 30 min	KOH 3:1 *w*/*w*, impregnation	10 °C·min^{-1} to 700 °C, hold 1 h	1231	0.54
			$ZnCl_2$ 3:1 *w*/*w*, impregnation	10 °C·min^{-1} to 600 °C, hold 1 h	1303	0.56
			KOH 3:1 *w*/*w*, impregnation	10 °C·min^{-1} to 400 °C, hold 1 h	470	0.25
				10 °C·min^{-1} to 500 °C, hold 1 h	1491	0.62
				10 °C·min^{-1} to 600 °C, hold 1 h	1885	0.78
				10 °C·min^{-1} to 700 °C, hold 1 h	2010	0.82
				10 °C·min^{-1} to 800 °C, hold 1 h	1909	0.92
			KOH 1:1 *w*/*w*, impregnation	10 °C·min^{-1} to 700 °C, hold 1 h	984	0.43
			KOH 2:1 *w*/*w*, impregnation		1605	0.66
			KOH 4:1 *w*/*w*, impregnation		1949	0.84
			KOH 5:1 *w*/*w*, impregnation		2380	1.14
			KOH 6:1 *w*/*w*, impregnation		2379	1.29
[16]	Waste cork stoppers	Carbonization under N_2, 10 °C·min^{-1} to 600 °C, 2 h	H_2SO_4		180	0.08
[17]	Cork stoppers pulverized to <900 µm	Carbonisation under N_2, 100 mL·min^{-1}, 5 °C·min^{-1} to 800 °C, 1 h		N_2, 100 mL·min^{-1}, 5 °C·min^{-1} to 900 °C, hold 1 h	1149	0.96
			NH_3	N_2, 100 mL·min^{-1}, 5 °C·min^{-1} to 700 °C, switch to NH_3, hold 1 h	558	0.36
				N_2, 100 mL·min^{-1}, 5 °C·min^{-1} to 800 °C, switch to NH_3, hold 1 h	1022	0.68
				N_2, 100 mL·min^{-1}, 5 °C·min^{-1} to 900 °C, switch to NH_3, hold 1 h	2060	2.21
[25]	Cork granulates (0.25–0.45 mm)	Carbonization under N_2, 550 °C, 1 h	KOH 3:1 *w*/*w*, solid mixing	N_2, 750 °C, 2 h	2567	1.16
			KOH 4:1 *w*/*w*, solid mixing		2707	1.28
			KOH 5:1 *w*/*w*, solid mixing		2865	1.43
[34]	Cork powder	Carbonization under N_2, 300 mL·min^{-1}, 10 °C·min^{-1}, 550 °C, 1 h	KOH 5:1 *w*/*w*, solid mixing	650 °C, 2 h	2422	1.09
				750 °C, 2 h	2948	1.37
				850 °C, 1 h	3072	1.57
				850 °C, 1.5 h	3246	1.81
				850 °C, 2 h	3403	2.07

There has been a significant improvement in the properties of activated carbons using two-step pyrolysis processes; one of the most recent studies could achieve an excellent surface area of 3403 $m^2 \cdot g^{-1}$, which is the highest so far reported for cork-based carbon materials, using KOH as the activating agent at a ratio of 5:1 to cork [34]. This area value is higher than the 3000 $m^2 \cdot g^{-1}$ reported as the highest achievement for the two-step production of activated carbons using other lignocellulosic biomass sources [27]. Zhang et al. [24] note that thermal pretreatment, even at temperatures as low as 350 °C, causes a thinning of the cell walls, thereby making them more permeable to the activating agent and increasing the development of micro and mesoporosity. The activation process also enables the opening of the porosity by washing away or preventing the formation of the molten tar accumulated in the honeycomb structure after pyrolysis [18,20,34]. Interestingly, along the wide range of activating methodologies used, the increase in the pyrolysis temperature fosters the development of microporosity up to temperatures of around 600 °C [23,24], while above this level, mesoporosity is enhanced, enabling the formation of a hierarchical pore structure [25]. The synergy between macro, meso and micropores facilitates diffusion of the adsorbate through the carbon structure, leading to fast access to the adsorption sites [25].

Some researchers attribute the development of mesoporosity due to the presence of gaseous physical activating agents [17,19,22]. Alternative approaches, such as using NH_3 [17] and air [22], were also applied to create surface characteristics such as amino groups, for the former and oxygen-containing groups, for the latter.

5. Applied Biosorption with Cork-Based Materials

Sorption using cork, either natural or modified into biochar or activated carbon, can be applied in a variety of pollutants (heavy metals, organic pollutants) as well as different states of matter (liquid, gas). This section discusses the comparative performance of these biosorption applications for each type of pollutant.

5.1. Biosorption of Metals

Biosorption of toxic metals in their cationic form, namely "heavy metals", as they are commonly known, had already been thoroughly explored at the beginning of the century, as previously reported [3]. In the last ten years, research on the adsorption of inorganic ions using cork adsorbents has shifted to anionic compounds, which had not yet been the object of study.

Some studies early in the decade have still reported the adsorption of cationic metals cadmium [36] and mercury [37]. The findings align with previous research on the biosorption of toxic metals using cork biomass; in the latter study, authors have even found that using recycled cork stoppers as the material did not present any significant differences from raw cork byproducts. The optimum pH for adsorption is in the neutral range, avoiding the competition with H^+ that occurs for more acidic values. Lopes et al. [37] have demonstrated for the first time that ion exchange is part of the adsorption mechanism for metal uptake in cork biomass, at least partly; they have shown that the extent of Hg^{2+} adsorbed is equivalent to the amount of Ca^{2+} and K^+ released in the same amount of time, in the first stage of the adsorption reaction. Furthermore, the adsorption kinetics are well described by the pseudo-second-order [36,37] and Elovich [37] models; the isotherm is well described by the Langmuir model in the case of cadmium [36]. Maximum adsorption capacities obtained with a Langmuir model fit are presented in Table 4.

In the case of mercury, Lopes et al. [37] have observed an unusual type III isotherm derived from increased removal efficiency for high initial concentrations, which enables an easy achievement of an equilibrium concentration of 20–30 $\mu g \cdot L^{-1}$ regardless of the pollutant load. Still, the adsorption capacity for lower equilibrium concentrations is deficient. These authors have also studied mercury adsorption in different aqueous matrixes, namely in a binary Hg/Cd system and in seawater. They found that cork is more selective towards

Hg than Cd, with minimal interference of the latter, while in seawater, Hg adsorption was much more reduced due to the formation of Hg chloro-complexes.

Table 4. Langmuir maximum adsorption capacities obtained in metal biosorption by cork and cork-derived biosorbents.

Source	Pollutant	Size (mm)/Modification	pH	Solid/Liquid Ratio ($g \cdot L^{-1}$)	Initial Concentration ($mg \cdot L^{-1}$)	Langmuir r^2	q_{max} ($mg \cdot g^{-1}$)	
[36]	Cd(II)	<0.08 mm	6	1	10–100	0.996	9.65	(20 °C)
						0.996	12.48	(30 °C)
						0.996	14.77	(40 °C)
[38]	Cr(VI)	regranulated (300 °C steam heated), 0.25–0.42 mm	2	6.67	25–1000	0.994	22.98	
[39]	As(III)	iron-coated, 0.8–1.0 mm	9	2.5	1–40	0.978	4.9 ± 0.3	
[40]	Sb(III)	iron-coated, 0.8–1.0 mm	6	2.5	1–40	0.953	5.8 ± 0.5	
	Sb(V)		3			0.912	12 ± 2	
[41]	As(V)	iron-coated, 0.5–1.0 mm	3	2.5	1–40	0.997	5.8 ± 0.1	(10 °C)
						0.996	6.2 ± 0.2	(20 °C)
						0.999	6.9 ± 0.1	(30 °C)

Krika et al. [36] have also presented a thermodynamic study of metal adsorption onto cork biomass for the first time, concluding that Cd(II) adsorption was spontaneous and endothermic, with maximum adsorption capacity increasing with temperature (Table 4).

Regarding anionic pollutants, our previous review had already reported some studies about Cr(VI) adsorption onto raw cork biomass [3]. Since then, Sfaksi et al. [42] have published new results on the same topic and Şen et al. [38] on regranulated cork, which is steam-treated at around 300 °C to produce agglomerate, for the same purpose. New studies have also emerged on the adsorption of As, Sb and P oxyanions using a novel modified cork biosorbent coated with iron [39,43,44]

As expected, unlike cationic metals, the anions are adsorbed more easily at acidic pH since electrostatic attraction may be involved in their uptake; the functional groups are positively charged in this pH range, while the adsorbate is negatively charged [39,42]. In Cr(VI) adsorption, reduction to Cr(III) by reaction with the organic matter in cork must also be factored in; Şen et al. [38] have shown, however, that this is minimized with thermal treatment. In the adsorption of As and Sb, speciation must be considered. For the pentavalent forms (As(V) and Sb(V)), it was observed that adsorption was favoured at acidic pH because they are negatively charged starting at pH as low as 2. However, for the trivalent forms (As(III) and Sb(III)), the neutral form predominates through the acidic and neutral range, and therefore the neutral pH is preferred [39,44].

It was found that the kinetics of anion adsorption were also well described by the pseudo-second-order and Elovich models; the former for Cr(VI) [42] and As(III) [39], and the latter for As(V) [39], Sb(III), Sb(V), and P(V) [43,44]. These indicate that the process occurs by chemisorption or on a multilayer in a heterogeneous surface. For iron-coated cork granulates, the adsorption occurs on the coating rather than the cork structure, and this coating is not homogeneous [39].

The reported equilibrium isotherms reinforce the fact that adsorption occurs on a multilayer. While some successful adjustments of the Langmuir model have been presented for Cr(VI) [38], As(III) [39], As(V) [41], Sb(III), and Sb(V) [44], enabling the calculation of maximum adsorption capacities (Table 4), the Freundlich model presents equal or superior fits for the adsorption of As(V), Sb(III), Sb(V), and P(V) [39,43,44]. Sfaksi et al. [42] report an unusual type IV isotherm for the adsorption of Cr(VI), with a good fit of the BET model.

Pintor et al. [40,44] have also studied the adsorption of As(III), As(V), Sb(III), Sb(V), and P(V) in the presence of electrolytes, such as NaCl or KNO_3. The increased ionic strength

caused different effects on the pollutants: when adsorption decreased, like for As(III) and Sb(V), it meant that electrostatic attraction played a part in the uptake; when adsorption was maintained or even increased, like for As(V), Sb(III), and P(V), the adsorption mechanism was chiefly inner-sphere complexation. Further studies with the same material and the pentavalent forms of these anions [43] showed competitive behaviour in binary and ternary solutions, with As(V) and Sb(V) suffering the highest interference by the other pnictogens while P(V) was more affected by the presence of other ions in the form of electrolytes.

A thermodynamic study of As(V) adsorption onto iron-coated cork granulates was carried out by Carneiro et al. [41]. The reaction was spontaneous and endothermic, and the adsorption capacity increased with temperature (Table 4). Sfaksi et al. [42] also showed a slight increase in Cr(VI) adsorption capacity by cork biomass with temperature.

Carneiro et al. [45] have also studied the desorption of As(V) from iron-coated cork granulates using NaOH 0.01 M and 0.1 M, being able to reuse the adsorbent for 3 to 4 cycles of adsorption, both in batch and continuous modes.

Finally, a recent development has been the production of biochar from cork powder, aiming to increase the material's porosity and adsorption potential by a simple procedure of slow pyrolysis. Wang et al. [23] have produced such biochars and applied them to Cu(II) adsorption with good results. They were able to develop microporosity without damaging the cork's alveolar structure, increasing the surface area. This effect was increased with the pyrolysis temperature and correlated positively with the adsorption capacity towards the studied metal.

5.2. Biosorption of Organic Pollutants

Cork, either as is or transformed into biochars or activated carbon, has been used for biosorption of a series of organic pollutants such as industrial dyes [46], phenol and derivatives [46] and emergent pollutants such as antibiotics [47] or herbicides/pesticides [48].

Table 5 summarizes the maximum uptake values obtained for those pollutants on cork and derivates (such as biochar or activated carbon prepared from cork) reported in the literature, derived from fitting the Langmuir model to experimental results.

Due to a limited number of studies, few cross-referenced interpretations can be made with accuracy. Regardless, some indications can be seen from the comparison of studies described in Table 5.

For instance, it is expected that the smaller the cork particles, the larger the surface area and, therefore, higher adsorption. Although that certainly is the case at pH 9 in Crespo-Alonso et al. [47], the same cannot be said at pH 4, and in Nurchi et al. [49], a lower q_{max} can be found for chrysoidine G at pH 7 at a lower cork granulometry. It is hypothesized that the sorption is not merely a surface phenomenon but dependent on the weight of the sorbent [47].

pH is also a relevant parameter which seemingly increases the q_{max} of some pollutants, such as ofloxacin and chrysoidine G when compared directly in the studies analysed. pH is relevant as it affects the protonation equilibria of the pollutants [47], which can enhance or limit the adsorption depending on the interactions between cork particles and said protonation species of each pollutant. Additionally, pH may also affect the surface charge of the sorbent if ion exchange is an important adsorption mechanism [49].

By analyzing Table 5, it can be seen that ofloxacin and chrysoidine G are the pollutants that were more easily adsorbed while using unaltered cork residues. However, such interpretations must be considered with proper care due to significant experimental design differences between studies that heavily limit comparisons. For instance, some values of chrysoidine G adsorption come after cork powder entrapment in a biopolymeric gel of calcium alginate, which seemingly increases adsorption capacity, although it increases equilibrium time, in particular at pH values where cork adsorption is lower.

Another relevant aspect is the adsorption kinetics, as time may be of essential importance for potential future applications. In Machado et al. [50], cork granulates adsorbed 50% of Furosemide within 24 h, being faster (as well as having higher q_{max}) than the other tested

sorbent, Low Expanded Clay Aggregates (LECA), and also being seemingly independent on initial concentration. In this case, cork granulates could be used to enhance wetland system efficiency for this type of pharmaceutical active compounds, either alone or in combination, based on adsorption capacity.

Table 5. Organic pollutant removal by adsorption to raw cork or biochar produced from cork.

Source	Pollutant	Size (mm)/Activation Method	pH	Solid/Liquid Ratio ($g \cdot L^{-1}$)	Initial Concentration ($mg \cdot L^{-1}$)	Langmuir r^2	q_{max} ($mg \cdot g^{-1}$)
[47]	ofloxacin	0.42–0.841 & >0.42	4	12.5	181–1806	-	31.1
		>0.42	9				37.9
		0.42–0.841	9				24.9
[50]	furosemide	-	-	150	1–11	0.183	0.25
[51]	phenol	<2	6	20	5–50	0.98	0.92
	2-chlorophenol					0.99	1.54
	2-nitrophenol					0.99	5.09
	2,4-dichlorophenol					0.94	6.24
	pentachlorophenol			10		0.95	5.31
[46]	methyl orange	<0.08	2	5	100	0.996	16.66
[52]	fuchsin or basic violet 14	0.63–0.75	6	6.66	100	0.979	29.9
[48]	carbamazepine	3–4	-	100	1–35	0.878	0.37
	clofibric acid					0.870	0.06
	Ibuprofen					0.876	0.32
[49]	chrysoidine G	>0.42	4	12.5	-	-	36.3
		>0.42 (in alginate)					42.4
		0.42–0.841	7				44.6
		>0.42					57.3
		>0.42 (in alginate)					61.5
[53]	fluoxetine	<1	9	0.1–1.5	5	0.884	10 ± 3
Biochar or activated carbon (AC) produced from cork							
[25]	methylene blue	Two-step carbonization under N_2 and KOH activation 3:1 w/w	-	1	100–1800	1.000	806.4
		Two-step carbonization under N_2 and KOH activation 4:1 w/w				1.000	990.1
		Two-step carbonization under N_2 and KOH activation 5:1 w/w, 750 °C				1.000	1059.8
[35]	methylene blue	<75 µm, activated with alkaline wastewater and carbonization under N_2	-	2–3.5	10–700	0.902	333.33
[34]	methylene blue	Two-step carbonization under N_2 and KOH activation 5:1 w/w, 850 °C	-	0.25	50–2500	0.997	1283.99
	rhodamine B					0.982	4067.57
	methyl orange					0.992	2666.2
	congo red					0.997	8920.6
[19]	ibuprofen	steam activation, carbonization under N_2	5	0.2–0.67	20–150	0.995	143.1
		KOH activation, carbonization under N_2				0.993	174.4

In the case of the pollutants studied by Mallek et al. [51], the adsorption of phenolic compounds reached an equilibrium in five minutes. Desorption was not observed for these compounds. It was also found that the higher the electronegativity of the substituting groups in the aromatic ring, the greater the sorption capacity of the cork, as seen in Table 5.

Other trends in the kinetic adsorption of organic pollutants by cork can also be found: Krika and Benlahbib [46] found that the adsorption rate of methyl orange has a decreasing trend with increasing initial concentration as well as solution temperature. However, higher capacity was also found with increasing concentration.

From the recent advances in the research on the use of cork as a precursor for activated carbon and biochars, as mentioned in a previous section, multiple end uses have been studied, and for organic pollutant adsorption, only three studies with comparable data points were found. Compared to others in Table 5, all four studies, particularly those with similar pollutants, have a significantly higher value of q_{max}, which denotes the potential of carbonization and activation to enhance the adsorption capacity of cork in particular.

Wang et al. [25], Novais et al. [35] and Wang et al. [34] tested activated carbon from cork for methylene blue adsorption, but differences in preparation methods led to different surface areas (2865, 1670 and 3403 $m^2 \cdot g^{-1}$, respectively), which reflected in a different q_{max} (up to 1059.8, 333.33 and 1283.99 $mg \cdot g^{-1}$, respectively). However, kinetics was similar (between 5 and 10 min). Wang et al. [34] found high values of q_{max} also for rhodamine B, methyl orange and congo red.

Wang et al. [25] further tested desorption for sorbent regeneration, which was found to be possible, albeit with a reduction of capacity to half after three desorption-adsorption cycles, while Wang et al. [34] found regeneration efficiencies of ethanol elution after 5 cycles between 38.38% and 86.19%, depending on the dye.

Finally, Mestre et al. [19] tested the production of activated carbon with two different methodologies based on expanded corkboard rather than cork dust which might have influenced the obtained results. Regardless, it is clear that both methods yielded significantly higher q_{max} values for ibuprofen adsorption than the use of untreated cork in other studies [48].

Several studies hypothesize a wide variety of hypotheses regarding the adsorption mechanisms, some highly speculative. M À Olivella et al. [54] studied in detail the role of chemical components of cork in the sorption of several pesticides, where it was concluded that content in aliphatic extractives and phenolic extractives inhibit or favour sorption of all pesticides, respectively and that sorption of pesticides by cork is more suitable to hydrophobic pesticides with higher octanol-water partition coefficient and not adequate for hydrophilic pesticides. Although this aspect does not necessarily apply to all organic pollutants, it does provide some important insights into the mechanism of cork adsorption.

5.3. Biosorption of Gaseous Pollutants

Cork and its derivate products, such as activated carbons or biochars prepared with cork as a base material, can also potentially treat gaseous effluents. However, gaseous pollutant adsorption with cork materials is currently underexplored in practice and as a research topic. Atanes et al. [18] prepared and characterized waste cork powder-derived activated carbon for SO_2 adsorption. It was found that the activation type and temperature heavily influence adsorption, whereas higher surface area/porosity and surface basicity enhanced the uptake. Based on Freundlich isotherms, the authors found that the cork-derived activated carbon performed similarly to other activated carbons in the literature, such as lignite and oil-palm waste and lower than molecular sieves.

Cork-based activated carbon was also researched for VOC removal. Xu et al. [17] synthesized activated carbon by two-step carbonization with ammonia activation of cork stopper waste (Table 5), achieving abundant amounts of micro-mesopores. This activated carbon presented an adsorption performance of 1221 $mg \cdot g^{-1}$ for acetone at 18 kPa, 840 $mg \cdot g^{-1}$ for benzene at 10 kPa and 720 $mg \cdot g^{-1}$ for toluene at 3 kPa.

Another potential application is CO_2 capture. Zhang et al. [24] produced microporous carbon nanoflakes derived from biomass cork waste, achieving an adsorption capacity of 7.28 mmol g^{-1} at 0 °C and 1 bar and 4.27 mmol g^{-1} at 25 °C, values that are higher than the majority of carbon-based sorbents in the literature. The prepared nanoflakes also presented good reusability and high selectivity to CO_2. Most important for this review is that the observed adsorption capacity of the prepared nanoflakes was, in large part, due to the characteristics of the precursor material, i.e., cork, taking advantage of its unique properties such as the tightly stacked closed and hollow honeycomb cells of uniform size and thinner wall.

Although there is a very limited number of recent sources of cork-derived products for gaseous emission control, the innate characteristics of the material are shown to be of particular interest, and therefore more research on this topic should be developed.

6. Concluding Remarks

Significant advances in the research of adsorption applications for cork and cork-based materials have been reported in the last decade. Namely, the trend in biochar production has been analysed for different types of cork material, concluding that it presents advantages due to the uniqueness of its cellular structure.

Some progress has been made on cork powder and granulates' composition and imaging, but more information on its characteristics is needed to explore its potential fully. Namely, more advanced imaging techniques, such as neutron radiography and tomography, are yet to be applied to either cork powder or cork-derived sorbents. Reported use of these techniques for studying other biosorbents suggests a high potential to more fully characterize and, by extension, reveal improvement opportunities in the adsorption process.

Two-step pyrolysis processes, a novel approach tested on various biomass, have achieved exceptional results on cork, unlocking new porosity and surface area levels. Using carbonization at 550 °C followed by activation using KOH 5:1 w/w with solid mixing and second pyrolysis at 850 °C achieved the highest surface area value for a cork-based carbon material so far. The increase in surface area and porosity is good for adsorption applications and opens avenues in other areas, such as the production of carbon-based electrodes. Alternative approaches can also create specific surface characteristics of potential interest, such as amino- or oxygen-containing groups for specific adsorption needs.

Biosorption of heavy metals, organics and gaseous pollutants are all potential applications of cork-based materials, but many lines in these three topics are still open to new research. In terms of heavy metals, previous research had already been extensive on the use of raw cork granulates for cation adsorption, and new studies have revealed simple coatings and transformations for effective application in anion adsorption. Organic pollutants are a class of growing interest due to the rise in emerging pollutants of concern; however, despite some complementary studies with raw cork granulate applications, little progress has been made in this regard. The same applies to gaseous pollutants, of which only a study on VOC and another on CO_2 capture could be found.

We predict that the next decade will bring further advances in the applications of cork-based activated carbons now that their textural properties match those of many activated carbons used commercially. More studies on the removal of inorganic and organic micropollutants, including pharmaceuticals and personal care products, VOC adsorption, gas separation, and CO_2 capture, are needed to evaluate the practical value of the high levels of porosity and surface area that have recently been reached.

Author Contributions: Conceptualization, A.P. and J.J.; methodology, A.P. and J.J.; validation, R.N.d.S.; data curation, A.P. and R.N.d.S.; writing—original draft preparation, A.P. and J.J.; writing—review and editing, R.N.d.S.; All authors have read and agreed to the published version of the manuscript.

Funding: This work was funded by LA/P/0045/2020 (ALiCE), UIDB/50020/2020, UIDP/50020/2020 (LSRE-LCM), funded by national funds through FCT/MCTES (PIDDAC). CTCOR is funded by SIAC2021: Scientific and technological interface. Cork industry (POCI-01-0246-FEDER-181298) and CTCOR—Innovation and Technological Centre—CTI basal funding (AAC nº 03/C05-i02/2022). A. Pintor acknowledges her Junior Researcher contract by FCT (CEECIND/01485/2017) and R. Nunes da Silva her Researcher contract by PORNorte (NORTE-06-3559-FSE-0000112).

Data Availability Statement: Data available on request.

Conflicts of Interest: The authors declare no conflict of interest.

References

1. Rives, J.; Fernandez-Rodriguez, I.; Rieradevall, J.; Gabarrell, X. Integrated environmental analysis of the main cork products in southern Europe (Catalonia–Spain). *J. Clean. Prod.* **2013**, *51*, 289–298. [CrossRef]
2. Gil, L. New Cork-Based Materials and Applications. *Materials* **2015**, *8*, 625–637. [CrossRef] [PubMed]
3. Pintor, A.M.A.; Ferreira, C.I.A.; Pereira, J.C.; Correia, P.; Silva, S.P.; Vilar, V.J.P.; Botelho, C.M.S.; Boaventura, R.A.R. Use of cork powder and granules for the adsorption of pollutants: A review. *Water Res.* **2012**, *46*, 3152–3166. [CrossRef] [PubMed]
4. Oliveira, G.; Costa, A. How resilient is *Quercus suber* L. to cork harvesting? A review and identification of knowledge gaps. *For. Ecol. Manag.* **2012**, *270*, 257–272.
5. APCOR, Cork as a Building Material Technical Manual. Available online: https://www.apcor.pt/wp-content/uploads/2015/07/Caderno_Tecnico_F_EN.pdf (accessed on 15 May 2023).
6. Sierra-Pérez, J.; Boschmonart-Rives, J.; Dias, A.C.; Gabarrell, X. Environmental implications of the use of agglomerated cork as thermal insulation in buildings. *J. Clean. Prod.* **2016**, *126*, 97–107. [CrossRef]
7. Crouvisier-Urion, K.; Bellat, J.-P.; Gougeon, R.D.; Karbowiak, T. Mechanical properties of agglomerated cork stoppers for sparkling wines: Influence of adhesive and cork particle size. *Compos. Struct.* **2018**, *203*, 789–796. [CrossRef]
8. Silva, S.P.; Sabino, M.A.; Fernandes, E.M.; Correlo, V.M.; Boesel, L.F.; Reis, R.L. Cork: Properties, capabilities, and applications. *Int. Mater. Rev.* **2005**, *50*, 345–365. [CrossRef]
9. Pereira, H. Variability of the chemical composition of cork. *Bioresources* **2013**, *8*, 2246–2256. [CrossRef]
10. Lagorce-Tachon, A.; Mairesse, F.; Karbowiak, T.; Gougeon, R.D.; Bellat, J.-P.; Sliwa, T.; Simon, J.-M. Contribution of image processing for analysing the cellular structure of cork. *J. Chemom.* **2018**, *32*, e2988. [CrossRef]
11. Crouvisier-Urion, K.; Chanut, J.; Lagorce, A.; Winckler, P.; Wang, Z.; Verboven, P.; Nicolai, B.; Lherminier, J.; Ferret, E.; Gougeon, R.D.; et al. Four hundred years of cork imaging: New advances in the characterization of the cork structure. *Sci. Rep.* **2019**, *9*, 19682. [CrossRef]
12. Lagorce-Tachon, A.; Karbowiak, T.; Loupiac, C.; Gaudry, A.; Ott, F.; Alba-Simionesco, C.; Gougeon, R.D.; Alcantara, V.; Mannes, D.; Kaestner, A.; et al. The cork viewed from the inside. *J. Food Eng.* **2014**, *149*, 214–221. [CrossRef]
13. Berezovska, I.; Fettaka, H.; Salmon, T.; Toye, D.; Lodewyckx, P. Redistribution of a mixture of organic vapours inside an activated carbon filter. *Chem. Eng. J.* **2015**, *280*, 677–681. [CrossRef]
14. Sharma, K.; Bilheux, H.Z.; Walker, L.M.H.; Voisin, S.; Mayes, R.T.; Kiggans, J.O., Jr.; Yiacoumi, S.; DePaoli, D.W.; Dai, S.; Tsouris, C. Neutron imaging of ion transport in mesoporous carbon materials. *Phys. Chem. Chem. Phys.* **2013**, *15*, 11740–11747. [CrossRef]
15. Motte, J.-C.; Delenne, J.-Y.; Barron, C.; Dubreucq, É.; Mayer-Laigle, C. Elastic properties of packing of granulated cork: Effect of particle size. *Ind. Crops Prod.* **2017**, *99*, 126–134. [CrossRef]
16. Bhatia, S.K.; Gurav, R.; Choi, T.-R.; Kim, H.J.; Yang, S.-Y.; Song, H.-S.; Park, J.Y.; Park, Y.-L.; Han, Y.-H.; Choi, Y.-K.; et al. Conversion of waste cooking oil into biodiesel using heterogenous catalyst derived from cork biochar. *Bioresour. Technol.* **2020**, *302*, 122872. [CrossRef]
17. Xu, X.; Guo, Y.; Shi, R.; Chen, H.; Du, Y.; Liu, B.; Zeng, Z.; Yin, Z.; Li, L. Natural Honeycomb-like structure cork carbon with hierarchical Micro-Mesopores and N-containing functional groups for VOCs adsorption. *Appl. Surf. Sci.* **2021**, *565*, 150550. [CrossRef]
18. Atanes, E.; Nieto-Márquez, A.; Cambra, A.; Ruiz-Pérez, M.C.; Fernández-Martínez, F. Adsorption of SO_2 onto waste cork powder-derived activated carbons. *Chem. Eng. J.* **2012**, *211–212*, 60–67. [CrossRef]
19. Mestre, A.S.; Pires, R.A.; Aroso, I.; Fernandes, E.M.; Pinto, M.L.; Reis, R.L.; Andrade, M.A.; Pires, J.; Silva, S.P.; Carvalho, A.P. Activated carbons prepared from industrial pre-treated cork: Sustainable adsorbents for pharmaceutical compounds removal. *Chem. Eng. J.* **2014**, *253*, 408–417. [CrossRef]
20. Şen, A.U.; Nobre, C.; Durão, L.; Miranda, I.; Pereira, H.; Gonçalves, M. Low-temperature biochars from cork-rich and phloem-rich wastes: Fuel, leaching, and methylene blue adsorption properties. *Biomass Convers. Biorefinery* **2020**, *12*, 3899–3909. [CrossRef]
21. Nobre, C.; Şen, A.; Durão, L.; Miranda, I.; Pereira, H.; Gonçalves, M. Low-temperature pyrolysis products of waste cork and lignocellulosic biomass: Product characterization. *Biomass Convers. Biorefinery* **2021**, *13*, 2267–2277. [CrossRef]
22. Ren, S.; Deng, L.; Zhang, B.; Lei, Y.; Ren, H.; Lv, J.; Zhao, R.; Chen, X. Effect of Air Oxidation on Texture, Surface Properties and Dye Adsorption of Wood-Derived Porous Carbon Materials. *Materials* **2019**, *12*, 1675. [CrossRef] [PubMed]
23. Wang, Q.; Lai, Z.; Mu, J.; Chu, D.; Zang, X. Converting industrial waste cork to biochar as Cu(II) adsorbent via slow pyrolysis. *Waste Manag.* **2020**, *105*, 102–109. [CrossRef] [PubMed]

24. Zhang, X.; Elsayed, I.; Song, X.; Shmulsky, R.; Hassan, E.B. Microporous carbon nanoflakes derived from biomass cork waste for CO_2 capture. *Sci. Total Environ.* **2020**, *748*, 142465. [CrossRef]
25. Wang, Q.; Lai, Z.; Luo, C.; Zhang, J.; Cao, X.; Liu, J.; Mu, J. Honeycomb-like activated carbon with microporous nanosheets structure prepared from waste biomass cork for highly efficient dye wastewater treatment. *J. Hazard. Mater.* **2021**, *416*, 125896. [CrossRef] [PubMed]
26. Wang, Q.; Chu, D.; Luo, C.; Lai, Z.; Shang, S.; Rahimi, S.; Mu, J. Transformation mechanism from cork into honeycomb–like biochar with rich hierarchical pore structure during slow pyrolysis. *Ind. Crops Prod.* **2022**, *181*, 114827. [CrossRef]
27. Braghiroli, F.L.; Bouafif, H.; Neculita, C.M.; Koubaa, A. Influence of Pyro-Gasification and Activation Conditions on the Porosity of Activated Biochars: A Literature Review. *Waste Biomass Valorization* **2020**, *11*, 5079–5098. [CrossRef]
28. Chun, Y.; Lee, S.K.; Yoo, H.Y.; Kim, S.W. Recent advancements in biochar production according to feedstock classification, pyrolysis conditions, and applications: A review. *Bioresources* **2021**, *16*, 6512–6547. [CrossRef]
29. Bong, C.P.C.; Lim, L.Y.; Lee, C.T.; Ong, P.Y.; Klemeš, J.J.; Li, C.; Gao, Y. Lignocellulosic Biomass and Food Waste for Biochar Production and Application: A Review. *Chem. Eng. Trans.* **2020**, *81*, 427–432.
30. Suliman, W.; Harsh, J.B.; Abu-Lail, N.I.; Fortuna, A.-N.; Dallmeyer, I.; Garcia-Perez, M. Influence of feedstock source and pyrolysis temperature on biochar bulk and surface properties. *Biomass Bioenergy* **2016**, *84*, 37–48. [CrossRef]
31. Ochai-Ejeh, F.O.; Bello, A.; Dangbegnon, J.; Khaleed, A.A.; Madito, M.J.; Bazegar, F.; Manyala, N. High Electrochemical Performance of Hierarchical Porous Activated Carbon Derived from Lightweight Cork (*Quercus suber*). *J. Mater. Sci.* **2017**, *52*, 10600–10613. [CrossRef]
32. Ochai-Ejeh, F.O.; Momodu, D.Y.; Madito, M.J.; Khaleed, A.A.; Oyedotun, K.O.; Ray, S.C.; Manyala, N. Nanostructured Porous Carbons with High Rate Cycling and Floating Performance for Supercapacitor Application. *AIP Adv.* **2018**, *8*, 55208. [CrossRef]
33. Nabais, J.M.V.; Ledesma, B.; Laginhas, C. Removal of Amitriptyline from Aqueous Media Using Activated Carbons. *Adsorpt. Sci. Technol.* **2012**, *30*, 255–263. [CrossRef]
34. Wang, Q.; Luo, C.; Lai, Z.; Chen, S.; He, D.; Mu, J. Honeycomb-like Cork Activated Carbon with Ultra-High Adsorption Capacity for Anionic, Cationic and Mixed Dye: Preparation, Performance and Mechanism. *Bioresour. Technol.* **2022**, *357*, 127363. [CrossRef]
35. Novais, R.M.; Caetano, A.P.F.; Seabra, M.P.; Labrincha, J.A.; Pullar, R.C. Extremely Fast and Efficient Methylene Blue Adsorption Using Eco-Friendly Cork and Paper Waste-Based Activated Carbon Adsorbents. *J. Clean. Prod.* **2018**, *197*, 1137–1147. [CrossRef]
36. Krika, F.; Azzouz, N.; Ncibi, M.C. Adsorptive Removal of Cadmium from Aqueous Solution by Cork Biomass: Equilibrium, Dynamic and Thermodynamic Studies. *Arab. J. Chem.* **2016**, *9*, S1077–S1083. [CrossRef]
37. Lopes, C.B.; Oliveira, J.R.; Rocha, L.S.; Tavares, D.S.; Silva, C.M.; Silva, S.P.; Hartog, N.; Duarte, A.C.; Pereira, E. Cork Stoppers as an Effective Sorbent for Water Treatment: The Removal of Mercury at Environmentally Relevant Concentrations and Conditions. *Environ. Sci. Pollut. Res.* **2014**, *21*, 2108–2121. [CrossRef]
38. Şen, A.U.; Olivella, M.À.; Fiol, N.; Miranda, I.; Villaescusa, I.; Pereira, H. Removal of Chromium (VI) in Aqueous Environments Using Cork and Heat-Treated Cork Samples from *Quercus cerris* and *Quercus suber*. *Bioresources* **2012**, *7*, 15. [CrossRef]
39. Pintor, A.M.A.; Vieira, B.R.C.; Santos, S.C.R.; Boaventura, R.A.R.; Botelho, C.M.S. Arsenate and Arsenite Adsorption onto Iron-Coated Cork Granulates. *Sci. Total Environ.* **2018**, *642*, 1075–1089. [CrossRef]
40. Pintor, A.M.A.; Vieira, B.R.C.; Boaventura, R.A.R.; Botelho, C.M.S. Removal of Antimony from Water by Iron-Coated Cork Granulates. *Sep. Purif. Technol.* **2020**, *233*, 116020. [CrossRef]
41. Carneiro, M.A.; Pintor, A.M.A.; Boaventura, R.A.R.; Botelho, C.M.S. Efficient Removal of Arsenic from Aqueous Solution by Continuous Adsorption onto Iron-Coated Cork Granulates. *J. Hazard. Mater.* **2022**, *432*, 128657. [CrossRef]
42. Sfaksi, Z.; Azzouz, N.; Abdelwahab, A. Removal of Cr(VI) from Water by Cork Waste. *Arab. J. Chem.* **2014**, *7*, 37–42. [CrossRef]
43. Pintor, A.M.A.; Brandão, C.C.; Boaventura, R.A.R.; Botelho, C.M.S. Multicomponent Adsorption of Pentavalent As, Sb and P onto Iron-Coated Cork Granulates. *J. Hazard. Mater.* **2021**, *406*, 124339. [CrossRef] [PubMed]
44. Pintor, A.M.A.; Vieira, B.R.C.; Brandão, C.C.; Boaventura, R.A.R.; Botelho, C.M.S. Complexation Mechanisms in Arsenic and Phosphorus Adsorption onto Iron-Coated Cork Granulates. *J. Environ. Chem. Eng.* **2020**, *8*, 104184. [CrossRef]
45. Carneiro, M.A.; Coelho, J.F.R.; Pintor, A.M.A.; Boaventura, R.A.R.; Botelho, C.M.S. Multi-cycle regeneration of arsenic-loaded iron-coated cork granulates for water treatment. *J. Water Process Eng.* **2022**, *50*, 103291. [CrossRef]
46. Krika, F.; Benlahbib, O.E.F. Removal of Methyl Orange from Aqueous Solution via Adsorption on Cork as a Natural and Low-Coast Adsorbent: Equilibrium, Kinetic and Thermodynamic Study of Removal Process. *Desalin. Water Treat.* **2015**, *53*, 3711–3723. [CrossRef]
47. Crespo-Alonso, M.; Nurchi, V.M.; Biesuz, R.; Alberti, G.; Spano, N.; Pilo, M.I.; Sanna, G. Biomass against Emerging Pollution in Wastewater: Ability of Cork for the Removal of Ofloxacin from Aqueous Solutions at Different PH. *J. Environ. Chem. Eng.* **2013**, *1*, 1199–1204. [CrossRef]
48. Dordio, A.V.; Gonçalves, P.; Texeira, D.; Candeias, A.J.; Castanheiro, J.E.; Pinto, A.P.; Carvalho, A.J.P. Pharmaceuticals Sorption Behaviour in Granulated Cork for the Selection of a Support Matrix for a Constructed Wetlands System. *Int. J. Environ. Anal. Chem.* **2011**, *91*, 615–631. [CrossRef]
49. Nurchi, V.M.; Crespo-Alonso, M.; Biesuz, R.; Alberti, G.; Pilo, M.I.; Spano, N.; Sanna, G. Sorption of Chrysoidine by Row Cork and Cork Entrapped in Calcium Alginate Beads. *Arab. J. Chem.* **2014**, *7*, 133–138. [CrossRef]
50. Machado, A.I.; Dordio, A.; Fragoso, R.; Leitão, A.E.; Duarte, E. Furosemide Removal in Constructed Wetlands: Comparative Efficiency of LECA and Cork Granulates as Support Matrix. *J. Environ. Manag.* **2017**, *203*, 422–428. [CrossRef]

51. Mallek, M.; Chtourou, M.; Portillo, M.; Monclús, H.; Walha, K.; ben Salah, A.; Salvadó, V. Granulated Cork as Biosorbent for the Removal of Phenol Derivatives and Emerging Contaminants. *J. Environ. Manag.* **2018**, *223*, 576–585. [CrossRef]
52. Olivella, M.À.; Fiol, N.; de la Torre, F.; Poch, J.; Villaescusa, I. Assessment of Vegetable Wastes for Basic Violet 14 Removal: Role of Sorbent Surface Chemistry and Porosity. *Desalin. Water Treat.* **2015**, *53*, 2278–2288. [CrossRef]
53. Silva, B.; Martins, M.; Rosca, M.; Rocha, V.; Lago, A.; Neves, I.C.; Tavares, T. Waste-Based Biosorbents as Cost-Effective Alternatives to Commercial Adsorbents for the Retention of Fluoxetine from Water. *Sep. Purif. Technol.* **2020**, *235*, 116139. [CrossRef]
54. Olivella, M.À.; Bazzicalupi, C.; Bianchi, A.; Fiol, N.; Villaescusa, I. New Insights into the Interactions between Cork Chemical Components and Pesticides. The Contribution of π–π Interactions, Hydrogen Bonding and Hydrophobic Effect. *Chemosphere* **2015**, *119*, 863–870. [CrossRef]